Proceeding of the 2013
RSI/ISMInternational Conference on Robotics and Mechatronics
February 13-15, 2013, Tehran, Iran

Dynamic Analysis and Control Synthesis of a Spherical Wheeled Robot (Ballbot)

Amin Lotfiani
Department of Mechanical Engineering
Isfahan University of Technology
Isfahan, Iran
a.lotfiani@me.iut.ac.ir

Mehdi Keshmiri
Department of Mechanical Engineering
Isfahan University of Technology
Isfahan, Iran
mehdik@cc.iut.ac.ir

Mohamad Danesh
Department of Mechanical Engineering
Isfahan University of Technology
Isfahan, Iran
danesh@cc.iut.ac.ir

Abstract— **Ballbot is a mobile robot consists of a body mounting on a spherical wheel. The spherical wheel can make the robot move in any directions. This robot is an unstable underactuated system with nonholonomic velocity constraints. In this paper, first, a 3D dynamic model of the robot is derived while taking the nonholonomic constraints into considerations. Since Ballbot is an underactuated system, finding a normal form for the equations could be helpful in the control point of view. Therefore, the equations of motion are examined to find whether there is a simple normal form or not. To enforce the robot to track any given trajectory on the ground, an online fuzzy logic trajectory planning is suggested. A computed torque method and a sliding mode controller are used along the fuzzy trajectory planning to perform the tracking goal. To consider uncertainties and disturbances, some simulations are performed. The results show that the sliding mode controller demonstrate much better performance compared to the computed torque controller. When there is no uncertainty, the computed torque method is candidate showing less tracking error than the sliding controller.**

Index Terms— **Ballbot, Moving mobile, Wheeled inverted pendulum, Nonholonomic systems**

I. INTRODUCTION

Stabilization problem of cart-pendulum system has been investigated both theoretically and practically extensively [1-3]. Ballbot introduced in [4] is actually an inverted pendulum mounted on a spherical wheel (Fig. 1). As shown in Fig. 2, the wheel receives its motion from the drive motors which are installed in the cylindrical body. The capability of moving in different directions without turning around, in addition to some other features like compact size, light weight and convenient in moving through narrow ways, has attracted some researchers to study this spherical wheeled robot recently. The balance control of Ballbot using LQR [4] and fuzzy controller [5] has been investigated, assuming planar motion for the system. Since uncertainties do exist in real situation, the fuzzy controller has resulted in better performance in practical. Besides balancing problem, an offline trajectory planning is also proposed in [6] to move the ballbot between two static situations. In order to keep the robot upright in static situations, system with hydraulic legs has been designed in [7].

It should be noted that in all the previous, Ballbot has been modeled as a 2D dynamic system. Although the planar model of the ballbot is valuable, but the spatial analysis is more reliable in practical situations. Besides, in study of the controlled system, linear controllers have been used. These controllers show appropriate performance if the body of the robot deviates slightly from the upright position. This is not the condition when the robot affected by large external disturbances or robot is under a fast maneuver. Therefore, designing a nonlinear controller for the system seems to be inevitable.

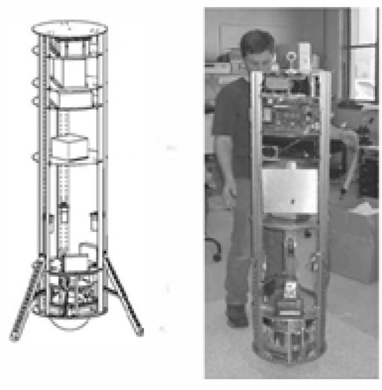

Fig. 1. Ballbot [4]

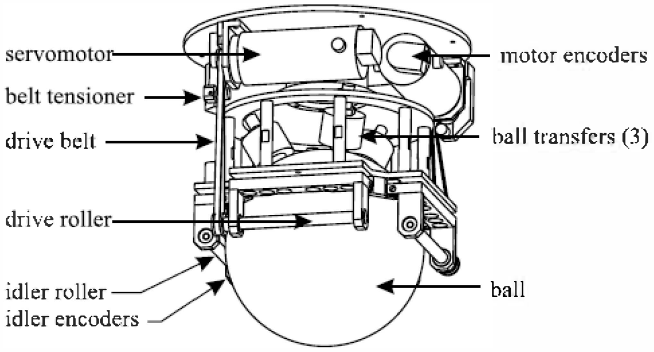

Fig. 2. Drive mechanism of Ballbot [4]

The main focus of this paper is to model the 3D motion of the Ballbot robot and introduce a robust nonlinear control method to track given trajectories on the ground.

As mentioned before, Ballbot is an underactuated system. Since the number of control inputs in underactuated systems, are fewer than the generalized coordinates, the control of these kinds of systems is more complicated. Important features of underactuated systems such as controllability, accessibility and stabilization are discussed in [8-10]. Finding an explicit change of coordinates and control inputs that transform several classes of underactuated systems, in the field of robotics and aerospace, into cascade nonlinear systems is addressed in [11]. The structural properties of the new formulation are more convenient for control design purposes. Due to complexity of the Ballbot dynamics, using the methods discussed in [11] to find a simple normal form for the equations of motion could be very helpful.

In this paper, initially we derive a 3D dynamic model of the Ballbot in order to deal with the real situations. Then the equations are examined to find whether there is a simple normal form or not. After that a fuzzy logic method is introduced to plan desired trajectories for the body angles, following by proposition of two different controllers (sliding mode and computed torque method) to track the trajectories. Numerical simulations are used to verify the performance of the closed loop system.

II. 3D Dynamic Model

In order to study the 3D motion of the Ballbot, the following assumptions are made: (1) There is no slip between the ball and the floor, (2) the contacting rollers between the body and the sphere are always in contact with the ball, (3) the cylinder center of gravity is located on its longitudinal axis, (4) the ball is completely symmetric.

To describe the dynamics of the robot, three $X_0 Y_0 Z_0$ inertial frame, $X_c Y_c Z_c$ body attached frame, and $X_s Y_s Z_s$ sphere attached frame are introduced (Fig. 3). The angular velocity of the cylinder with respect to inertial frame ($\vec{\omega}_c$) can be obtained by three consecutive rotations θ_c, ϕ_c and ψ_c about X_0, Y_0 and Z_0. Similarly, the angular velocity of the sphere ($\vec{\omega}_s$) can be obtained by three rotations θ_s, ϕ_s, and ψ_s .

Now we can define the generalized coordinates as $q=[\theta_c\ \phi_c\ \psi_c\ \theta_s\ \phi_s\ \psi_s]^T$ to describe the system dynamics. It should be noted that considering the above mentioned assumptions, the system has only four degrees of freedom (DOF). This means the configuration space of the system is described by six generalized coordinates which are related by two nonholonomic constraints [12].

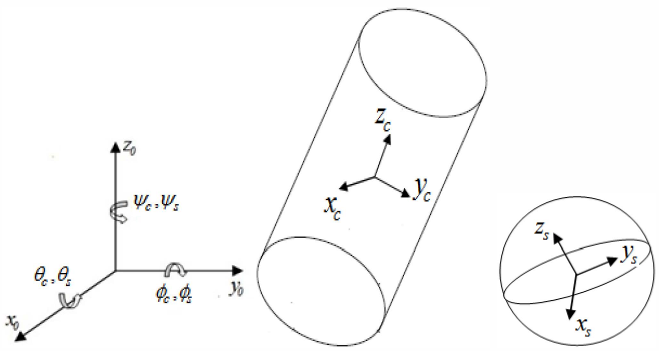

Fig. 3. Inertial and fixed bodies' frames

These constraints are extracted by assuming the resultant moment around cylinder longitudinal axis to be equal to zero. Therefore components of angular velocities of the sphere and the cylinder along the cylinder longitudinal axis are zero, i.e.

$$\begin{aligned}&\dot{\theta}_c \sin(\phi_c) - \dot{\phi}_c \cos(\phi_c)\sin(\theta_c)\\ &\qquad + \dot{\psi}_c \cos(\phi_c)\cos(\theta_c) = 0\end{aligned} \tag{1}$$

and

$$\begin{aligned}&\dot{\theta}_s \sin(\phi_c) - \dot{\phi}_s \cos(\phi_c)\sin(\theta_c)\\ &\qquad + \dot{\psi}_s \cos(\phi_c)\cos(\theta_c) = 0.\end{aligned} \tag{2}$$

To derive the equations we need to calculate the friction forces exerted by the driving rollers and idler rollers (Fig. 2). Denoting τ_1 and τ_2 as the deriving torques, and ignoring the roller inertia, the friction force of active rollers are given by

$$\vec{F}_{c_i} = \frac{|\vec{\tau}_i|}{r_r}\hat{v}_i \qquad i = 1,2, \tag{3}$$

where r_r is the radius of the rollers. The unit vector $\hat{v}_i$ is calculated by the following equations:

$$\begin{aligned}\hat{v} &= \frac{\vec{V}_{rel}}{(\vec{V}_{rel}\,.\vec{V}_{rel})^{1/2}},\\ \vec{V}_{rel} &= \vec{V}_{P_i} - \vec{V}_{P_i'} = (\vec{\omega}_s - \vec{\omega}_c)\times \vec{r}_i \quad i = 1,2,\end{aligned} \tag{4}$$

where $\vec{V}_{P_i}$ and $\vec{V}_{P_i'}$ are the velocity of the corresponding contact points on the ball and cylinder and $\vec{r}_i$ is the vector that connects the center of the ball to each contact point.

The friction of the idle rollers is assumed to be modeled as viscous:

$$\vec{F}_{f_i} = 1/2\, c\,(\dot{q}_{c_i} - \dot{q}_{s_i})(\dot{q}_{c_i} - \dot{q}_{s_i})^T, \quad i = 1,2, \tag{5}$$

where c is the viscous damping coefficient between the ball and the idlers.

Using Lagrange equations for nonholonomic systems [13, 14] the equations of motion can be written as:

$$M(q)_{6\times 6}\,\ddot{q} + H(q,\dot{q})_{6\times 1} = B_{6\times 2}\,\tau_{2\times 1} + A^T{}_{6\times 2}\,\lambda_{2\times 1}, \tag{6}$$

where A is:

$$A = \begin{pmatrix} a_1 & a_2 & a_3 & 0 & 0 & 0 \\ 0 & 0 & 0 & a_1 & a_2 & a_3 \end{pmatrix} \qquad (7)$$

and $a_1 = sin\,\phi_c$, $a_2 = -cos\phi_c sin\theta_c$ and $a_3 = cos\phi_c cos\theta_c$.

The null space of $A(q)$ is given by the matrix $S(q)$, so the vector $\dot{q}$ has to lie in this null-space, i.e. we can consider a set of reduced generalized velocities, $\dot{q}_r$, where

$$\dot{q} = S\,\dot{q}_r\,. \qquad (8)$$

Next, we follow the standard procedure for the elimination of the Lagrange multipliers by pre-multiplication with S^T to obtain

$$M_r(q)_{4\times4}\,\ddot{q}_r + H_r(q,\dot{q})_{4\times1} = B_r(q,\dot{q})_{4\times2}\,\tau_{2\times1}\,, \qquad (9)$$

where

$$\begin{aligned} &M_r(q) = S^T M(q) S\,, \\ &H_r(q,\dot{q}) = S^T(M\dot{S}\,\dot{q}_r + H(q,\dot{q})), \\ &B_r = S^T B(q,\dot{q}). \end{aligned} \qquad (10)$$

The equations in (9) suffer from input coupling [11]. In order to deal with this problem we define $q' = [\theta_c\ \phi_c\ \psi_c\ \theta_s'\ \phi_s'\ \psi_s']^T$ and $q_r' = [\theta_c\ \phi_c\ \theta_s'\ \phi_s']^T$, where $\theta_s' = \theta_c - \theta_s$, $\phi_s' = \phi_c - \phi$ and $\psi_s{}' = \psi_c - \psi_s$. Using these new definitions, the equations of motion can be presented in the following form,

$$M'(q')_{4\times4}\,\ddot{q}_r' + H'(q',\dot{q}')_{4\times1} = B'(q',\dot{q}')_{4\times2}\,\tau_{2\times1}\,. \qquad (11)$$

By inspection, one can realize that Eq. 11 can be written as

$$M_{cc}'(q')\,\ddot{q}_{r_c}' + M_{cs}'(q')\,\ddot{q}_{r_s}' + H_c'(q',\dot{q}') = 0 \qquad (12)$$

and

$$M_{sc}'(q')\,\ddot{q}_{r_c}' + M_{ss}'(q')\,\ddot{q}_{r_s}' + H_s'(q,\dot{q}) = B_s'(q',\dot{q}')\tau, \qquad (13)$$

where $q_{r_s}' = [\theta_s'\ \phi_s']$ and $q_{r_c}' = [\theta_c\ \phi_c]$.

It should be noted that because of long terms, it is not possible to mention the equations of motion extensively in this paper and more details can be found in [15].

III. Normal Form of the Equations of Motion

Since the equations of motion of the 3D model are so complex, finding a simple normal form could be very useful for the purpose of control.

According to [11], the necessary and sufficient condition of the existence of a global change of coordinates that transforms the system to a simple normal form is:

$$\frac{\partial g_0^j(q)}{\partial q_1} g_0^i(q) - \frac{\partial g_0^i(q)}{\partial q_1} g_0^j(q) + \frac{\partial g_0^j(q)}{\partial q_2}\,\frac{\partial g_0^i(q)}{\partial q_2} = 0, \forall i, j = 1,..,m, \qquad (14)$$

where for the system under consideration

$$g_0(q') = -M_{cc}'^{-1}(q')M_{cs}'(q') = (g_0^1(q), \ldots, g_0^m(q)) \qquad (15)$$

and $q_1 = q_{r_c}' = [\theta_c\ \phi_c]$, $q_2 = q_{r_s}' = [\theta_s'\ \phi_s']$, and m is the number of inputs. Using MAPLE, it is found that the Ballbot system does not satisfy Eq. 14. So, it is not possible to transfer the equations into a simple normal form. This means we have to try non analytical method to control the system.

IV. Online Trajectory Planning

Since Ballbot is an underactuated system it is not possible to control its all four degrees of freedom. This section is devoted to find a way to track the desired trajectory of the sphere, while the cylinder remains stable and does not collapse. In order to catch this purpose we use a fuzzy logic path generating block in addition to the control block.

The inputs of the fuzzy block are angular errors of the sphere and their derivatives. The outputs are the desired angles (the controller command angles) for the cylinder ($q_{r_c}^d$).

The closed loop of the system is shown in Fig. 4 and the fuzzy block is shown in detail in Fig. 5. Five membership functions are devoted for each input and nine membership functions for each output. The rules of two blocks are the same and considered as in table 1.

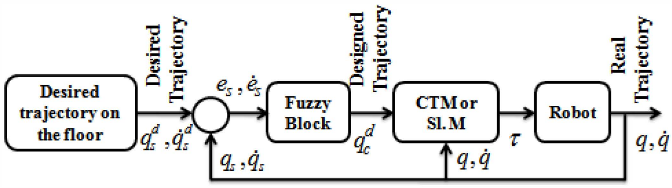

Fig. 4. Online trajectory planning and robot control

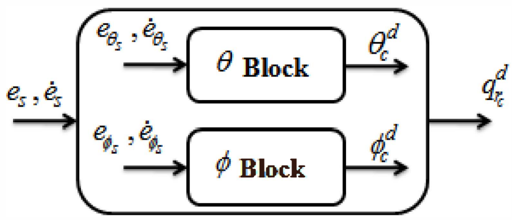

Fig. 5. Fuzzy block in detail

Table 1. Fuzzy rules

		$\dot{e}_s$				
	θ_c	*NB*	*NS*	*Z*	*PS*	*PB*
e_s	*NB*	NVB	NB	NM	NS	Z
	NS	NM	NM	NS	Z	PS
	Z	NM	NS	Z	PS	PM
	PS	NS	Z	PS	PS	PB
	PB	Z	PS	PM	NB	PB

V. Controller Design

The two control inputs are insufficient to control all the four joint variables. The controller is capable of controlling only two of them. The angular motion of the cylinder is selected for this purpose. The controller along with the fuzzy block tries to control the cylinder motion such that the sphere tracks the desired trajectory on the ground.

Two different controllers (a computed torque like controller and a sliding mode controller) are proposed for this purpose. The computed torque controller is given by

$$\tau = \bar{B}_c^{-1}(\bar{H}_c + \bar{M}_c(\ddot{q}_{r_c}^d + k_v(\dot{q}_{r_c}^d - \dot{q}_{r_c}) + k_p(q_{r_c}^d - q_{r_c}))), \qquad (16)$$

where

$$\bar{M}_c = (M'_{sc} - M'_{ss} M'^{-1}_{cs} M'_{cc}),$$
$$\bar{H}_c = (H'_s - M'_{ss} M'^{-1}_{cs} H'_c), \quad (17)$$
$$\bar{B}_c = B'_s$$

and k_p and k_v are positive definite diagonal matrices. The control law for the sliding mode approach is proposed as the following [16],

$$\tau = \hat{B}_c^{-1}(\hat{M}_c(\ddot{q}_{r_c}^d - \lambda\dot{\tilde{q}}_{c_r} - \eta\, sat(\frac{s}{\varphi})) + \hat{H}_c). \quad (18)$$

where

$$sat(\gamma) = \begin{cases} -1 & if\ \gamma < -1 \\ \gamma & if\ -1 < \gamma < 1 \\ 1 & if\ \gamma > 1 \end{cases} \quad (19)$$

and φ is a boundary layer thickness, η is a positive definite diagonal matrix and $\hat{M}_c$, $\hat{H}_c$ and $\hat{B}_c$ are the nominal values of the $\bar{M}_c$, $\bar{H}_c$ and $\bar{B}_c$ matrices.

VI. Results

Three different maneuvers are selected to evaluate performances of the proposed controllers. They are presented in the following subsections. For the simulation purposes similar values for physical parameter as those in [6] are used in this study (Table 2).

Table 2. Values of the physical parameters

Parameter	Value (unit)
Mass of the cylinder (m_c)	51.663 (kg)
Mass of the sphere (m_s)	2.473 (kg)
Radius of the sphere (r)	0.1 (m)
Center of mass of the cylinder	0.69 (m)
Moment of inertia of the cylinder about X_c axis	12.5 (kg.m^2)
Moment of inertia of the cylinder about Y_c axis	12.5 (kg.m^2)
Moment of inertia of the cylinder about Z_c axis	37.187 (kg.m^2)
Products of inertia of the cylinder	0
Moment of inertia of the sphere	0.018 (kg.m^2)
Radius of the rollers (r_r)	0.0064 (m)
Coefficient of viscous damping friction (c)	0.1 (N.m/rad/s)

For the parameter uncertainties the following are used in the simulations,

$$\hat{m}_c = 0.7\, m_c, \hat{m}_s = 0.7\, m_s, \hat{c} = 0.7\, c. \quad (20)$$

To study the capability of the controller in disturbance rejection, it is assumed that the cylinder is affected by following torque disturbances for duration of $\Delta t = 0.01 s$ at the specified time,

$$\tau'_x = 4.5\, N.m, \tau'_y = 5.5\, N.m. \quad (21)$$

A. Cylinder stabilization

In this section the performance of the CTM method in stabilizing the robot when the body experiences large angular motion is investigated. In this direction, the desired trajectory for the sphere is assumed as:

$$\theta_s^d = 0, \phi_s^d = 0. \quad (22)$$

This tries to retain the sphere at the origin. The following initial conditions for the cylinder are considered

$$\theta_c^0 = 0.2\, Rad, \phi_c^0 = 0.2\, Rad. \quad (23)$$

The simulation results for the closed loop system with the CTM controller for the undisturbed and disturbed cases are shown in figures 6 to 9. The disturbance is applied at $t = 10\, s$ and the gains of the controller are set as follows,

$$k_p = 64\, I_{2\times 2}, k_v = 16\, I_{2\times 2}. \quad (24)$$

B. Tracking a straight line

Performance of the proposed controllers in tracking the robot a given time trajectory on the ground is studied in this and the following sections. In this section tracking a straight line is considered,

$$x = r\,t, y = r\,t, \quad (25)$$

where r is the radius of the sphere. No slip condition enforces the following desired trajectories for the sphere,

$$\theta_s^d = t, \phi_s^d = t. \quad (26)$$

Two different situations are considered here. In the first one it is assumed that no disturbances affect the system and the system starts from zero initial conditions which is compatible with the desired conditions at $t = 0$. In the second one the cylinder is initially deviated from the upright position and the disturbances affect the system at $t = 10 s$. The initial conditions for the cylinder are assumed to be

$$\theta_c^0 = 0.2\, rad, \phi_c^0 = 0. \quad (27)$$

The controller gains are considered to be as those in (28) and the simulation result for these two cases are shown in Figs. 10 and 11,

$$\varphi = 0.01, \lambda = 22.33, I_{2\times 2}, \eta = 5.67\, I_{2\times 2},$$
$$k_p = 64\, I_{2\times 2}, k_v = 16\, I_{2\times 2}. \quad (28)$$

C. Tracking a circle

Instead of a line, the following circle is considered to be tracked on the ground by the Ballbot,

$$x = 2\sin(0.05t), \ y = 2\cos(0.05t). \quad (29)$$

The initial position of the sphere is assumed to be

$$x = 0, \ y = 2.22\,(m), \quad (30)$$

which means the robot is placed out of the desired trajectory at $t = 0$. It is also assumed that the disturbance is applied at $t = 20\, s$ and the controller parameters are set as

$$\varphi = 0.005, \lambda = 25.5\, I_{2\times 2}, \eta = 4\, I_{2\times 2},$$
$$k_p = 72.25\, I_{2\times 2}, \ k_v = 17\, I_{2\times 2}. \quad (31)$$

Figure 11 shows the simulation results for this case.

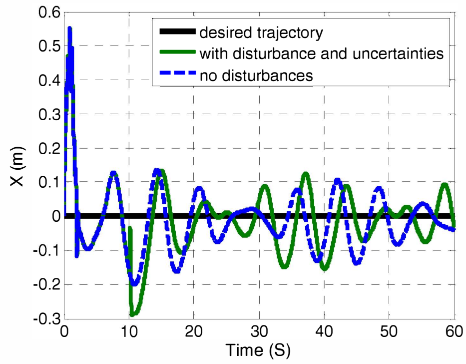

Fig. 6. Sphere motion in the x direction during the stabilization process

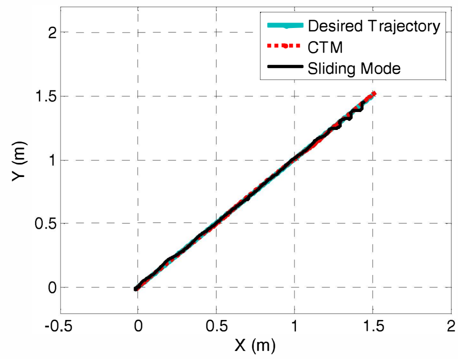

Fig. 10. Straight line tracking, no disturbances, compatible initial conditions

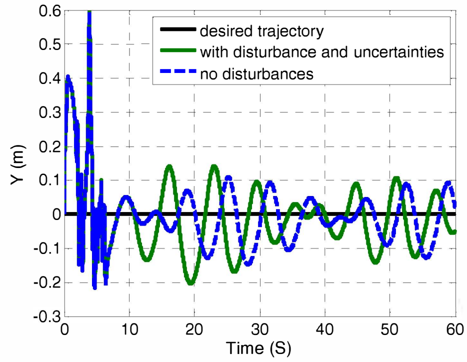

Fig. 7. Sphere motion in the y direction during the stabilization process

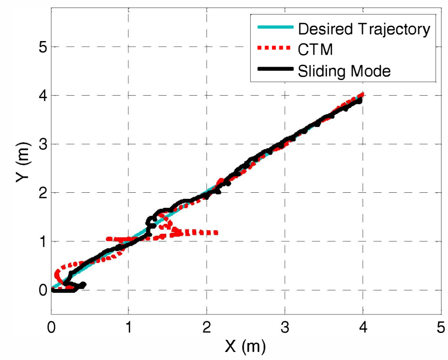

Fig. 11. Straight line tracking in the presence of disturbance and initial deviation of the cylinder

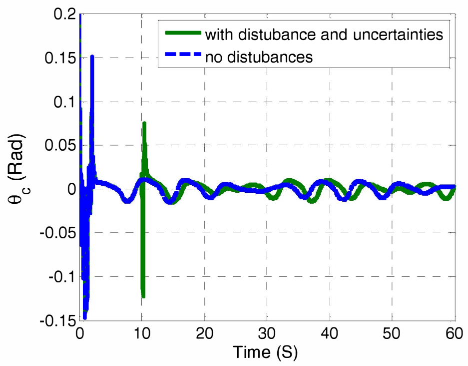

Fig. 8. Time history of the θ_c during the stabilization process

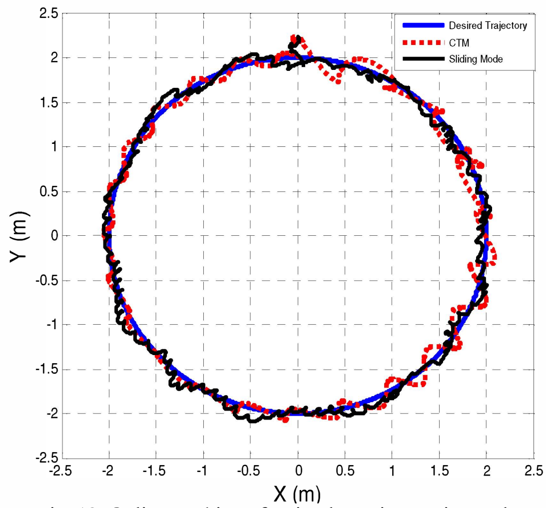

Fig. 12. Online tracking of a circular trajectory in xy plane

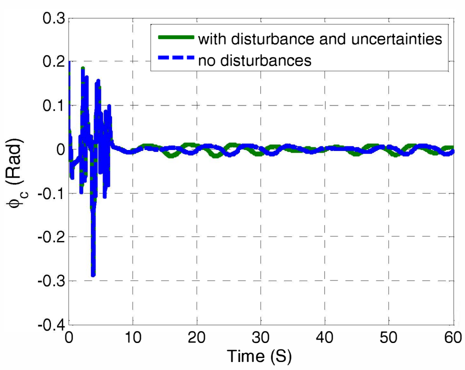

Fig. 9. Time history of the ϕ_c during the stabilization process

D. Discussion on results

As it is seen from Figs. 6 and 7 the nonzero initial condition of the cylinder causes the robot to move and get away from the origin. The controller computes the required torques such that fulfill both tasks; stabilizing the cylinder and bringing back the ball to the origin. Since the system is unstable, the final motion is an oscillatory motion around the origin. Effects of the disturbances can be obviously seen in Figs. 6-9. At $t = 10\,s$, when the disturbances are applied the green curves separated from the blue curves.

Figure 10 shows the controller is completely capable to track a straight line trajectory if there is no disturbance and no initial deviation. Comparing Figs. 10 and 11, the performance of the controller in rejecting the disturbances and eliminating the initial deviations is clearly understood. Similar trend is observed in Fig. 12 where the robot is supposed to track a curved trajectory such as a circle.

The advantage of the sliding mode controller to the CTM controller can be realized from the results shown Figs. 11 and 12. These figures depict that in the presence of any disturbance, the sliding mode controller is more capable in rejecting the disturbance.

It should be noted that since in the above cases the trajectory tracking of the ball on the ground and stabilization of the cylinder were set as the main purpose the controlling system, no efforts have been put in controlling the rotations of the cylinder and sphere around the vertical axis (ψ_c and ψ_s). They should only remain bounded. Their values can be calculated by constraint equations (Eqs.1 and 2).

VII. Conclusions

Nonholonomic spatial dynamics of the Ballbot robot as well as the controller design for this highly unstable robot was studied in this paper. The dynamic equations were split into two set of actuated and unactuated equations, where the actuated part was used to control the ball motion on the ground and the unactuated part was used to stabilize the cylinder around the upright position. For given desired trajectories a fuzzy logic approach based on the current positions and velocities of the sphere was introduced to generate the desired positions of the cylinder.

Sliding mode and CTM approaches were proposed to track the planned trajectories by the fuzzy block. The performance of the controllers in stabilizing the cylinder and moving the sphere on a given trajectory on the ground investigated numerically. Simulation results showed that both controllers are able to fulfill the required tasks. However, when there is some sort of disturbances in the system, either from an external source or internal source, the sliding mode controller is more capable than the CTM controller.

References

[1] T. S. Li and M. Y. Shieh, "Switching-type Fuzzy Sliding Mode Control of a Cart-Pole System," Mechatronics J., Vol. 10, pp. 91-109, 2000.

[2] Y. S. Kim, H. Kim and Y. K. Kwan, "Dynamic Analysis of a Nonholonomic Two-Wheeled Inverted Pendulum Robot," J. of Intelligent and Robotic Systems, Vol. 44, pp. 25-46, 2005.

[3] K. Pathak, K. J. Franch and S. K. Agrawal, "Velocity and Position Control of a Wheeled Inverted Pendulum by Partial Feedback Linearization," IEEE Trans. On Robotics, Vol. 21, pp. 505-513, 2005.

[4] B. Lauwers, G. A. Kantor and R. Hollis, "A Dynamically Stable Single-Wheeled Mobile Robot with Inverse Mouse-Ball Drive," In Proc. IEEE Int'l. Conf. On Robotics and Automation, pp. 2884-2889, 2006.

[5] Y. F. Peng, C. H. Chiu and W. R. Tsai, "Design of an Omni-Directional Spherical Robot Using Fuzzy Control," Proc. Multi Conference of Engineers and Computer Scientists, Hong Kong, March, 2009.

[6] U. Nagarajan and R. Hollis, "Trajectory Planning and Control of an Underactuated Dynamically Stable Single Spherical Wheeled Mobile Robot", Proc. IEEE Int'l. Conf. on Robotics and Automation, Kobe, Japan, pp. 3743-3749, May 2009.

[7] U. Nagarajan and R. Hollis, "State Transition, Balancing, Station Keeping, and Yaw Control for a Dynamically Stable Single Spherical Wheel Mobile Robot", Proc. IEEE Int'l. Conf. on Robotics and Automation, May 2009.

[8] H. J. Sussmann, "A General Theorem on Local Controllability," SIAM J. of Control and Optimization, Vol. 25, pp. 158-194, 1987.

[9] M. Reyhanoglu, V. D. Schaft and N. H. McClamroch, "Dynamics and Control of a Class of Underactuated Mechanical Systems," IEEE Trans. On Automatic Control, Vol. 44, pp. 1663-1671, 1999.

[10] K.Y. Wichlund, O. J. Sordalen and O. Egeland, "Control of vehicles with second-order nonholonomic constraints: Underactuated Vehicles," European Control Conf., Rome, Italy, pp. 3086-3091, 1995.

[11] R. Olfati-Saber, Nonlinear Control of Underactuated Mechanical Systems with Application to Robotics and Aerospace Vehicles, Ph.D. dissertation, Massachusetts Institute of Technology, February 2001.

[12] J. R. Ray, "Nonholonomic constraints," Am. J. Phys., no. 34, pp 406-408, 1966.

[13] A.F. D'souza, Advanced Dynamics Modeling and Analysis, 1st ed., Chap. 5, 1983, pp. 120– 140.

[14] M. W. Spong, S. Hutchinson and M. Vidyasagar, Robot Modeling and Control, 1st ed., Chap. 2, 2005, pp. 37-70.

[15] A. Lotfiani, Spatial Dynamic modeling and Control of an Underactuated Single Spherical Wheeled Mobile Robot, MSc. Thesis, Isfahan University of Technology, April 2012.

[16] J. E. Slotin and W. Li, Applied Nonlinear Control, 1st ed., Prentice Hall Englewood Cliffs, Newjersy, 1991, pp. 276-307.